DESIGN AND PROCESSING OF ADVANCED MATERIALS FOR PERSPIRABLE SKIN

M. Wang[1], C.-W. Chen[2], M. Lempke[1], T. Wong[3], P. Kwon[1]*
[1] Mechanical Engineering, Michigan State University, East Lansing, Michigan, U.S.A.,
[2] Mechanical Engineering, National Taiwan University, Taipei, Taiwan
[3] Mechanical Engineering, Alfred University, Alfred, New York, U.S.A.
* Corresponding author (pkwon@egr.msu.edu)

Keywords: *Zirconium Tungstate(ZrW_2O_8), Perspirable Skin, Coefficient of Thermal Expansion, Buckling, Functionally Graded Material(FGM), Anisotropy, Sintering*

ABSTRACT
A Thermal Protection System (TPS) is essential on reentry vehicles, such as space shuttles, to reduce the surface temperature during reentry into Earth's atmosphere. A perspirable skin design has been proposed to autonomously cool the surface. The design requires a shrink-fitting process of two materials with distinct Coefficients of Thermal Expansion (CTE) and utilizes the CTEs differential and in-plane deformation to generate a gap between the two materials. However, to achieve a higher capacity for self-cooling, a new design was proposed using an assembly of design shapes (called 'tiles'), which will buckle under an expected thermal loading. These tiles had uniquely designed CTEs, where each tile pushes other tiles in certain directions while shrinking in other directions to enable buckling to occur under a given thermal loading. Finite Element Analysis (FEA) was performed with a set of possible material properties for a feasibility study. A major effort is now being made to fabricate the designed tiles, some with anisotropic and/or gradient material properties. This paper also reports on the development of processing techniques. Several samples were made successfully by compacting, pre-sintering, machining and fully sintering ceramic powders and powder mixtures.

1 Introduction

Due to the frictional heating on the exterior surface of a reentry vehicle such as a space shuttle, a Thermal Protection System (TPS) is essential to protect the vehicle [1]. The resulting temperature on the surface of the vehicle can be elevated to a level as high as 1700°C [1, 2]. Presently, the thermal ablation/erosion and oxidization reaction of the current TPS is a major threat to the safety of the vehicle [3].

In this work, we report on a new TPS design with an improved self-cooling capability by mimicking the perspiration of the human body, thus calling the design 'Perspirable Skin.' Our original design consists of a core material shrink-fitted into a skin panel, such as Reinforced Carbon-Carbon (RCC) Composite. In our previous study, the cores were made of either pure ZrW_2O_8, or Functionally Graded Materials (FGMs) made of ZrW_2O_8 and ZrO_2. The choice of ZrW_2O_8 was made among many negative CTE materials due to its highly negative coefficient of thermal expansion in a wide range of temperatures. When the surface temperature increases, a gap between the core and the RCC forms due to the difference in thermal expansions. A compressed coolant gas onboard the vehicle is passed through this gap onto the surface to envelope the surface, which is expected to substantially reduce the surface temperature.

Due to the limitation of small dimensions imposed on this design, the gap between the core and RCC was not big enough to achieve a high rate of cooling. Therefore, we proposed a new concept utilizing buckling. After many design iterations, an assembly of specially designed 'tiles' has shown great potential. Finite Element Analysis (FEA) simulations were carried out to confirm the buckling action based on the materials being considered. This paper represents our effort to produce these unique tiles and their assembly.

2 Design of Buckling Structures

Through many design iterations, a set of tiles assembled shown in Fig. 1(a) has chosen. The designed tiles are made of various materials with positive (e.g.: ZrO_2 or ceramic fibers) and negative (e.g.: ZrW_2O_8) CTEs. To confirm the viability of the buckling action, a simulation was performed using

ABAQUS. For our preliminary design analysis, the material properties were calculated using the rules of mixture along with the volume weighted average of the phases' (matrix and dispersed phase) properties [4]. With a volume ratio between ZrW_2O_8 and ZrO_2 of 7:3, the material properties used in our simulation were calculated, and presented in Table 1. The material for the core tile (shown in green on Fig. 1(a)) was imposed with a positive CTE of $3e^{-6}$.

In the FEM simulation, the loading condition imposed was 800ºC at the top surface and 50ºC at the bottom surface. Concerning the boundary conditions, each tile had its own axis of rotation, which was fixed to the surrounding RCC. With such loading and boundary conditions, the simulation has been carried out and confirmed that the designed assembly of tiles buckle as shown in Fig. 1(b). The geometry and the buckling action are shown in Fig. 1 without the RCC skin.

Table.1. Material properties for the simulation

Using Simple ROM/IROM	Radial	Tangent
CTE (/°C)	5.4e-6	-6e-6
Thermal conductivity (W/m/K)	5.6	2.7
E (MPa)	15.92	5.63
Poisson's ratio	0.3	

3 Experimental materials and procedure

3.1 Materials

According to the simulation results, the tiles with CTEs varying in at least two directions are needed to produce the buckling. While the CTE in one direction should be positive, the CTE in another direction needs to be negative. Two methods of producing anisotropic/gradient materials are presented in Fig. 2. The first method combines ceramic powders with ceramic fibers. With the fibers arranged radially, a positive CTE can be obtained along the fiber direction. However, this approach was not successful due to the reaction and residual stresses created during sintering. Alternatively, arranging ZrO_2 and ZrW_2O_8 into certain shapes and sintering them together, creating a solid tile, can lead to different CTEs along different directions throughout the tile. Several ceramic powders and fibers that were used are shown in Table 2.

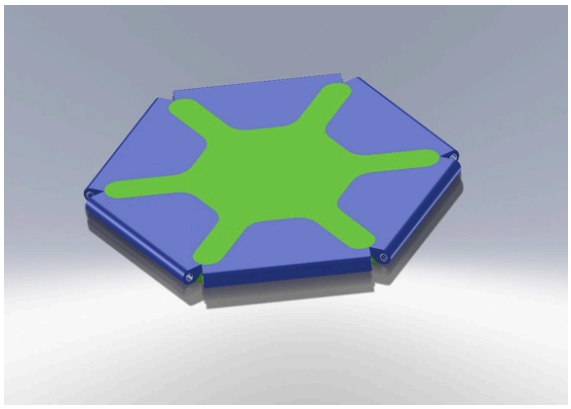

(a)

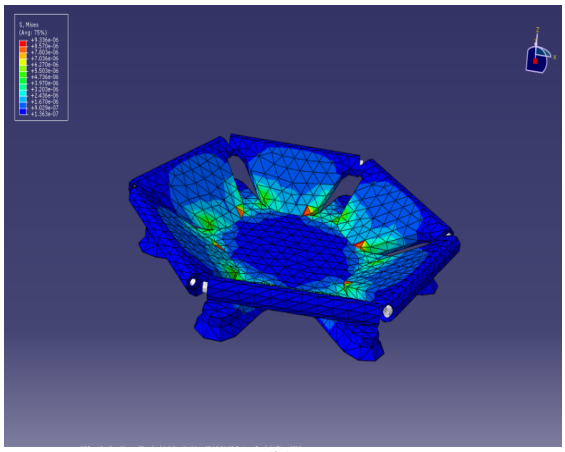

(b)

Fig.1. Buckling simulation: (a) original shape; (b) after buckling.

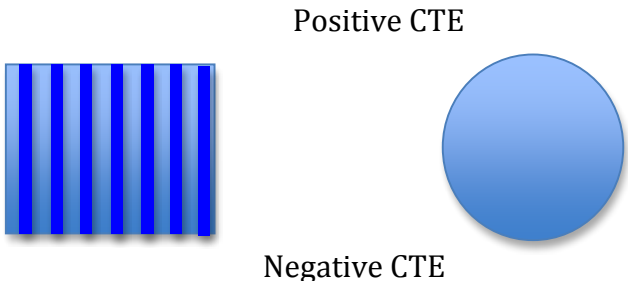

(a) (b)

Fig.2. Processing (a) ceramic powders with fibers; (b) Macroscopically FGM in radial Direction.

Table.2. Characteristics of Raw Powders used

Name	Material	Mean particle size (μm)	Manufacturer
W-Fluka	WO_3	8.22	Sigma-Aldrich, U.S.A.
CERAC-2003*	ZrO_2	1.23	CERAC Inc., U.S.A.
Nextel 610	Al_2O_3	½" chopped fiber	3M company
SCS-6	SiC	142	Specialty Materials, INC.

3.2 Procedure

3.2.1 Combination of ceramics and fibers

The WO_3+ZrO_2 powder mixture was mixed in a jar mill for 48 hours. The powder mixture with the stoichiometric ratio of WO_3 and ZrO_2 of 2:1 was prepared to attain pure ZrW_2O_8 [5]. With a small trace of Al_2O_3 powder, the final density of ZrW_2O_8 was improved [6]. Before mixing the powder with fibers, the fibers were heated to 600°C for two hours to remove the organic sizing [7]. The mixture was then stacked in a single-action die and chopped fibers were placed along one direction. The mixture was then compacted under 70MPa of pressure.

Green compacts were then sintered at 1150°C for 6 hours in a covered platinum crucible under the atmospheric pressure in a furnace (Carbolite-HTF1700, UK). The crucible provides a nearly sealed environment, which is essential to reduce the sublimation of WO_3 at temperatures higher than 800°C [8]. Since decomposition of ZrW_2O_8 occurs when the temperature drops below 1100°C, a quenching process, performed by removing the crucible from the furnace at the end of the soaking stage, provides rapid cooling and prevents the decomposition from occuring at a lower temperature.

3.2.2 Shrink-fitting Process to fabricate the assembly of ZrO_2 and ZrW_2O_8

Apart from the fabrication of the fiber-reinforced ZrW_2O_8, a shrink-fitting technique was used to fabricate the designed perspirable skin shown in Fig. 1. From our previous work [8], we were able to make FGMs made of ZrO_2 and ZrW_2O_8. However, the processing technique was limited to produce the gradiency in one direction (through-the-thickness) only. The arrangement shown in Fig. 2(a) provides anisotropy in a composite-like manner. With short chopped fibers arranged various ways within a matrix, a complex gradiency can be achieved. However, as will be shown in Sec. 4, the processing of these materials presented many problems.

Alternatively, the arrangement shown in Fig. 2(b) can be the tile used for the simulation in Fig. 1. However, for simplification purposes, a simple circle has been used instead of the tile shape shown in Fig. 1. The tiles denoted positive CTE and negative CTE can be the FGMs produced in our previous work [9]. The denoted positive and negative CTEs mean the macroscopic CTE of each FGM tile. Fig. 2(b) is capable of achieving a wide variety of CTEs radially depending on the shape of the tile denoted positive CTE. We have not optimized the shape at the point. However, the designed shape behaves similarly as the tile used in our simulation shown in Fig. 1. To make the tile into the shape shown in Fig. 1, two methods were considered. One method was to make the sample using certain dies with the specific dimensions of the design's shape, and the other method was to machine the sample after partially sintering, and then fully sinter it to obtain the final product. The latter method was utilized to make the multidimensional material, since it was very inconvenient to design specific dies for each sample.

The overall processing technique is presented in Fig. 3. The WO_3+ZrO_2 powder mixture was first partially sintered at 950°C for four hours, and subsequently CNC-milled, in order to obtain a certain shaped cavity in which a ZrO_2 tile was shrink-fitted. The ZrO_2 tile was partially sintered at 900°C for three hours, and then was machined into a designed shape. After machining, the sample was fully sintered under 1350°C for four hours and then inserted into the ZrW_2O_8 tiles. These two tiles were co-sintered at 1150°C for 3 hours. By controlling the dimension of each part during partial-sintering and subsequent full sintering, the shrink-fit process has produced a successful assembly when considering the combination of ZrW_2O_8 shrinkage and ZrO_2 expansion during the sintering process. A reaction layer was formed at the boundary between the ZrW_2O_8 and ZrO_2, which is helpful in bonding these two materials together. Despite of the reaction, as long as the macroscopic CTEs are maintained, the processed tile will function properly.

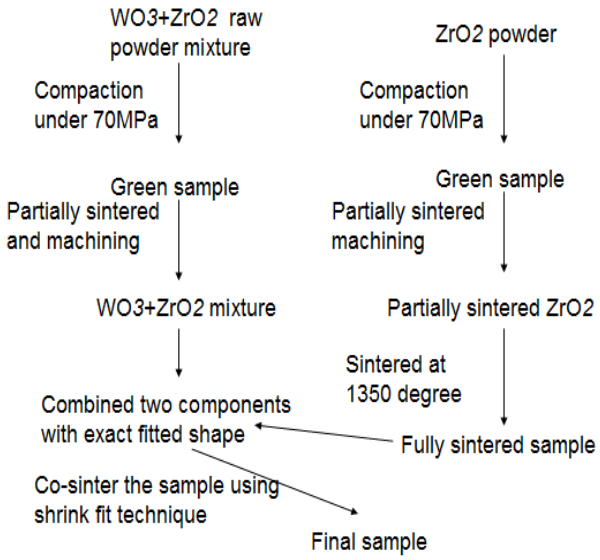

Fig.3. The Overall Processing Technique for shrink-fitting samples

4 Results and discussion

Concerning the combination of ZrW_2O_8 with fibers, it was found that Al_2O_3 fibers undergo a chemical reaction with WO_3 when the temperature is higher than 720°C [10]. This compound exists in a liquid phase above 1135°C, which destroys the shape of the sample. Therefore, because Nextel 610 was mostly composed by Al_2O_3, it was found to be unfit for our purposes.

SiC fibers are very stiff and stable. During the sintering process, SiC fibers also react with the WO_3+ZrO_2 mixture, and become a liquid mixture at temperatures over 1200°C. However, at a temperature of 1150°C, the sample maintains its shape, as shown in Fig. 4. The CTE value measured from the sample was found to be $-5.5X10^{-6}$, which is a slight increase of $1.5\ X10^{-6}$ compared with pure ZrW_2O_8. However, if we add more fibers to the mixture, the compaction of the green sample becomes a problem due to the stiffness of the SiC fibers, and the residual thermal stress due to the different CTE values will destroy the sample during the sintering process. Although there is no evidence of a chemical reaction between these two materials in our sample, the SiC fibers were not considered further.

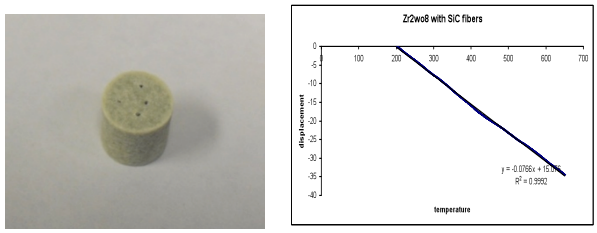

(a) (b)

Fig.4. Results for ZrW_2O_8 with SiC fibers: (a) sample; (b) CTE measurement data

The samples produced based on the procedure outlined in Fig. 3 are presented in Fig. 5; Fig. 5(a) is a simple version of our sample that did not require the machining of the ZrO_2 tile. ZrW_2O_8 was partially sintered, on which a hole was drilled. After 3 hours of co-sintering, the sample was shrink-fitted together by placing the fully sintered ZrO_2 into the hole drilled into the partially sintered ZrW_2O_8 disk.

Two obvious phenomena should be reported. From our previous paper [8], the ZrO_2 powder will undergo a reaction with WO_3+ZrO_2 mixture during the sintering process. From Fig. 5 (a), instead of the pure white color for the ZrO_2 powder, the core part has a yellow ring surrounding it, which is a mixture of ZrO_2 and ZrW_2O_8. Therefore, a functionally graded material was generated from the surrounding pure ZrW_2O_8 and the mixture of ZrO_2 and ZrW_2O_8 surrounding the pure ZrO_2. This FGM (the core part shown in Fig. 5 (a)) helps to join the two parts together. Adjusting the sintering temperature and soaking time can control the thickness of the reaction layer. The reaction layer is acceptable as long as the macroscopic CTEs are maintained.

Another important observation is the white spots on the ZrW_2O_8 tile. This is mostly due to the sublimation of WO_3 during the partial sintering and full sintering process, since it is known that the WO_3 powder will diffuse above 800°C. Therefore, the remaining ZrO_2 powders are the white spots shown on the surface. The sample shown in Fig. 5(b) is the tile used in our simulation shown in Fig. 1. Both ZrO_2 and ZrW_2O_8 were partially sintered and machined. The key part of this process is that we need to compensate the size change during the partial and full sintering processes. Then, the ZrO_2 sample will just fit into the shape after being fully

sintered. The reaction layer cannot be observed on Fig. 5(b) as the shrink-fit process has not taken place.

As presented with Fig. 2(b), the CTE along the major axis of the elliptical shape is positive while the CTE along the minor axis is negative. Given the material properties, the extent of the radial CTE variation is strictly a function of the exact shape of the ellipse. The elliptical shape was determined to match the CTE values presented in Table 1.

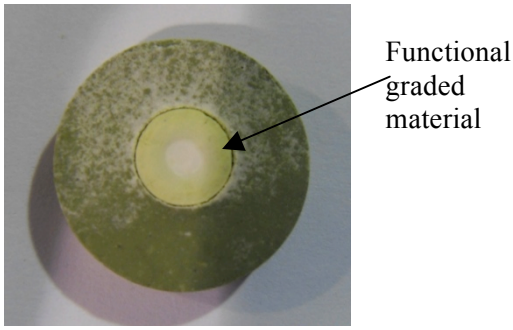

(a)

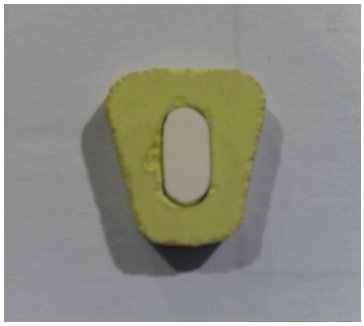

(b)

Fig.5. Shrink-fitting samples: (a) simple one with a ring shape; (b) a designed shape model to simulate the tile part in the simulation

The geometric shape of the sample (shown in Fig. 5(a)) was imported and simulated using COMSOL Multiphysics to evaluate the radial thermal expansion of the sample. This shape is chosen because TMA analysis can be readily carried out. The COMSOL result is shown in Fig. 6. The overall shape in Fig. 6 represents the deformation in all directions while the colors represent the displacement in the x-direction. The maximum displacement along radial direction is -6.037e-5, with a temperature change of 800K. Therefore, the CTE value evaluated by the COMSOL simulation is -3.95e-6. To verify the simulation results, the CTE values were also measured along two directions (shown in Fig. 6 as z-direction and r-direction using polar coordinates) using the TMA machine.

For the axial (z) direction, the CTE value was found to be 5e-6, which is close to the theoretical value of our ZrO_2 sample. The reason for the lower CTE value is the fact that the reacted FGM part will slightly offset the expansion of the ZrO_2 part. In the radial direction, the TMA measurement data is shown in Fig. 7, and the calculated value was found to be -3.5e-6. Compared with the simulation results, the higher CTE of the radial direction is mainly because of the sublimation of WO_3 during the partial and full sintering process. Instead of pure ZrW_2O_8, the final sintered sample turns out to be a mixture of ZrW_2O_8 and ZrO_2, which increases the CTE value. Despite of the reaction, the global CTE (both core and ring) measured using TMA was very close to the CTE calculated in COMSOL.

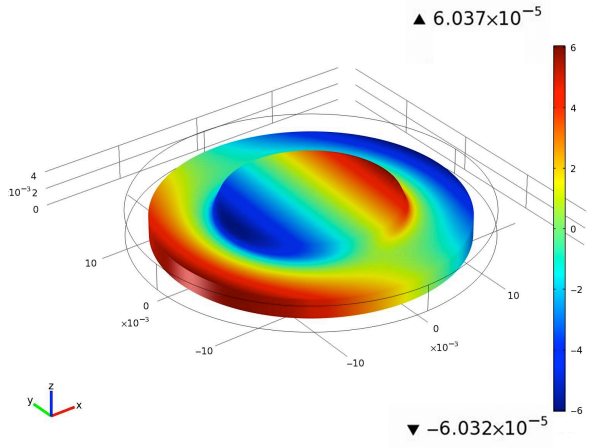

Fig.6. Simulation Result calculated by COMSOL.

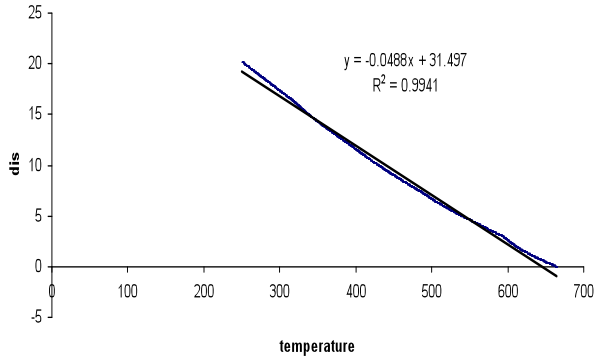

Fig.7. The radial CTE measurement data on the sample measured with TMA.

In order to have lower CTE values, one method is to sinter the sample in a furnace with a rich tungsten atmosphere, which will decrease the sublimation amount of WO_3. Another method is to reduce the amount of ZrO_2 involved in the sample, which inevitably increases the content of ZrW_2O_8 at the same time.

5. Conclusion

We proposed a tile, composed of several shrink-fit materials, in order to produce a buckling action on the assembly of these tiles under a given thermal loading. These tiles, seamlessly fit together, will expand or shrink, exerting forces on the other tiles, causing buckling when heated. The FEM simulation using ABAQUS verified that the model buckled downward by setting the proper design parameters and loading conditions. The successful processing method was the shrink-fitting technique described in this paper. It was found that ZrW_2O_8 undergos a chemical reaction with alumina fibers above 1135 degrees. The reaction compound $Al_2(WO_4)_3$ will change to a liquid phase, which distorts the final sample's shape, compromising the sample. Concerning SiC fibers, although there was no sign of a reaction with ZrW_2O_8, because of its stiffness and large CTE difference, the thermal stress during the sintering has broken the sample. Therefore, it is impossible to combine ZrW_2O_8 with fibers. By using the shrink-fitting technique, several samples were successfully made. ZrW_2O_8 and ZrO_2 tiles with a designed shape were partially sintered and machined, and with the dimension compensation, the perspirable skin assembly was fabricated. After co-sintering the sample, the tile was fabricated by controlling the sintering time. The CTE value was also measured to make a comparison with the results from FEA.

Acknowledgement

The authors acknowledge the support of Dr. Les Lee, the Program Manager for Mechanics of Multifunctional Materials & Microsystems at the U.S. Air Force Office of Scientific Research under the contract AFOSR FA9550-10-1-0238.

References

[1] J. A. Angelo, "The dictionary of space technology, New York: Facts on File". pp. 445-446, 1999.

[2] G. G. Cleland, 'Thermal protection system of the space shuttle, NASA contractor report: NASA CR-4227," 1989.

[3] G. Savage, "Carbon-carbon composites" New York: Chapman & Hall, pp. 37-80 & pp. 322-332, 1993.

[4] M. Taya, and R. Arsenault, "*Metal Matrix Composites".* 1st edition, Pergamon Press, 1989.

[5] L. Sun, X. Shi, A. Sneller, C. Uher and P. Kwon, "In-situ synthesis and thermal properties of ZrO_2/ZrW_2O_8," The proceeding for 23rd annual technical conference of ASC, pp. 14-23, 2008.

[6] L. Sun, and P. Kwon, "ZrW_2O_8/ZrO_2 composites by in situ synthesis of ZrO_2+WO_3: Processing, coefficient of thermal expansion, and theoretical model prediction". Material Science and Engineering Vol. A527, pp. 93-97, 2009.

[7] I.A.H. Al-Dawery, and E.G. Butler "Fabrication of high-temperature resistant oxide ceramic matrix composites". Composites Part A, Vol. 32, pp. 1007-1012, 2001.

[8] K. Kuribayashi, M. Yoshimura, T. Ohta, and T. Sata. "High-temperature phase relations in the system Y2O3-Y2O3·WO3" Journal of the American Ceramic Society, Vol. 63, No. 11-12, pp. 644-647, 1980.

[9] L. Sun and P. Kwon "ZrW_2O_8–ZrO_2 Continuous Functionally Graded Materials Fabricated by In Situ Reaction of ZrO_2 and WO_3". Journal of the American Ceramic Society, Vol. 93, No. 3, pp. 703-708, 2009.

[10] J.L. Waring "Phase equilibria in the system aluminum oxide/tungsten oxide". Journal of the American Ceramic Society, Vol. 48, No. 9, pp. 493-493, 1965.